Supporting Information

Tkatch et al. 10.1073/pnas.1703623114

SI Materials and Methods

Topology. In PM-localized ChR2, the C terminus (and thus the YFP tag) is known to face the cytoplasm. Accordingly, one would predict that in a functional IMM-localized channel the YFP tag should face the matrix. To determine whether indeed mitoChR2(SSFO)-YFP is localized in the IMM and with the correct topology, we carried out a sequential fluorescence quenching analysis as previously described (18). HeLa cells coexpressing the YFP-tagged mitoChR2(SSFO) and an OMM, N33D3cpv, or a matrix marker, 4mtD3cpv, were first treated with proteinase K (Fig. 2*A*). No significant drop in fluorescent signal was observed in the intact cells, indicating that all of the YFP tags are protected by the PM. Permeabilization of the PM by digitonin in the presence of proteinase K was followed, as expected, by a disappearance of N33D3cpv fluorescence (18), but neither the fluorescent signal of the matrix-localized 4mtD3cpv nor that of mitoChR2(SSFO)-YFP was affected. Similarly, trypan blue, a strong quenching agent for YFP that is permeable across the OMM, but not the IMM, had no effect on mitoChR2(SSFO)-YFP and 4mtD3cpv fluorescence. Finally, cells pretreated with digitonin were perfused with alamethicin, known to permeabilize both the OMM and IMM to high molecular weight solutes (19, 20). The 4mtD3cpv-associated fluorescent signal was almost completely lost, as expected for a matrix-soluble protein (Fig. 2*B*), but no change was observed in mitoChR2(SSFO)-YFP fluorescence, as predicted for a mitochondrial integral protein of the IMM. In the presence of alamethicin, however, trypan blue rapidly quenched mitoChR2(SSFO)-YFP fluorescence (Fig. 2*C*). Taken together, the above experiments indicate that (*i*) mitoChR2 is targeted exclusively to the IMM and does not reach the PM, and (*ii*) the YFP tag of these two constructs is neither exposed to the cytosolic surface of the OMM nor to the intermembrane space.

Aequorin Ca^{2+} Measurement. To strengthen and extend data about optogenetic control of mitochondrial Ca^{2+} uptake, we cotransfected mitoChR2(SSFO)-YFP, mitoChR2(SSFO), and mitoChR2(Tr) with mt-aequorin (or cyt-aequorin) to monitor the effect of channel opening on mitochondrial Ca^{2+} in a cell population. The data of Fig. S8*A* show that preilluminating the sample with blue light results in a strong reduction in the amplitude of the mitochondrial Ca^{2+} peak elicited by stimulation with IP_3-generating stimuli, compared with controls or cells expressing the truncated form of the channel. It is noteworthy that the average mitochondrial Ca^{2+} peaks of control cells with or without preillumination are indistinguishable (Fig. S8*B*), indicating that blue light is not inducing phototoxicity.

Given that aequorin is a chemiluminescent protein and emits light at 460 nm upon a rise in Ca^{2+} levels, the prediction is that the light emitted, locally, by aequorin during the Ca^{2+} rise may be sufficient in itself to open the channel and thus reduce the amplitude of the mitochondrial Ca^{2+} rise. Indeed, the data of Fig. S8*C* confirm that this is the case, namely that the peak amplitude of the mitochondrial Ca^{2+} rise even without preillumination was significantly diminished in cells expressing mitoChR2(SSFO)-YFP compared with controls. To confirm that the reduction is not due to an intrinsic toxicity due to channel expression but depends on the depolarization induced by mitoChR2(SSFO) opening, we induced a much smaller Ca^{2+} rise in mitochondria by activating capacitative Ca^{2+} entry (CCE) (47). Given that the aequorin light emission is not linearly but exponentially related to Ca^{2+} concentration, for a 10-fold reduction in the Ca^{2+} peak (as for CCE compared with a mix of stimuli) the reduction in light emitted is over 100-fold (Fig. S8*D*). As expected, thus, the peak amplitude of the mitochondrial Ca^{2+} rise due to CCE was indistinguishable in mitoChR2-YFP–expressing cells compared with controls, indicating that under these conditions the aequorin-emitted light is insufficient to significantly open the channel (Fig. S8*E*). Moreover, the cytosolic Ca^{2+} peak was induced by stimulation with the mix of stimuli (Fig. S8*F*) or through CCE induction (Fig. S8*G*). No differences between control cells and cells expressing mitoChR2(SSFO) were observed, corroborating the observation that no significant toxicity is caused by mitoChR2(SSFO) expression.

These results not only confirm the efficacy of mitoChR2(SSFO) in controlling mitochondrial Ca^{2+} uptake in a cell population but also demonstrate that the YFP-tagged and untagged ChR2 versions are indistinguishable and not toxic.

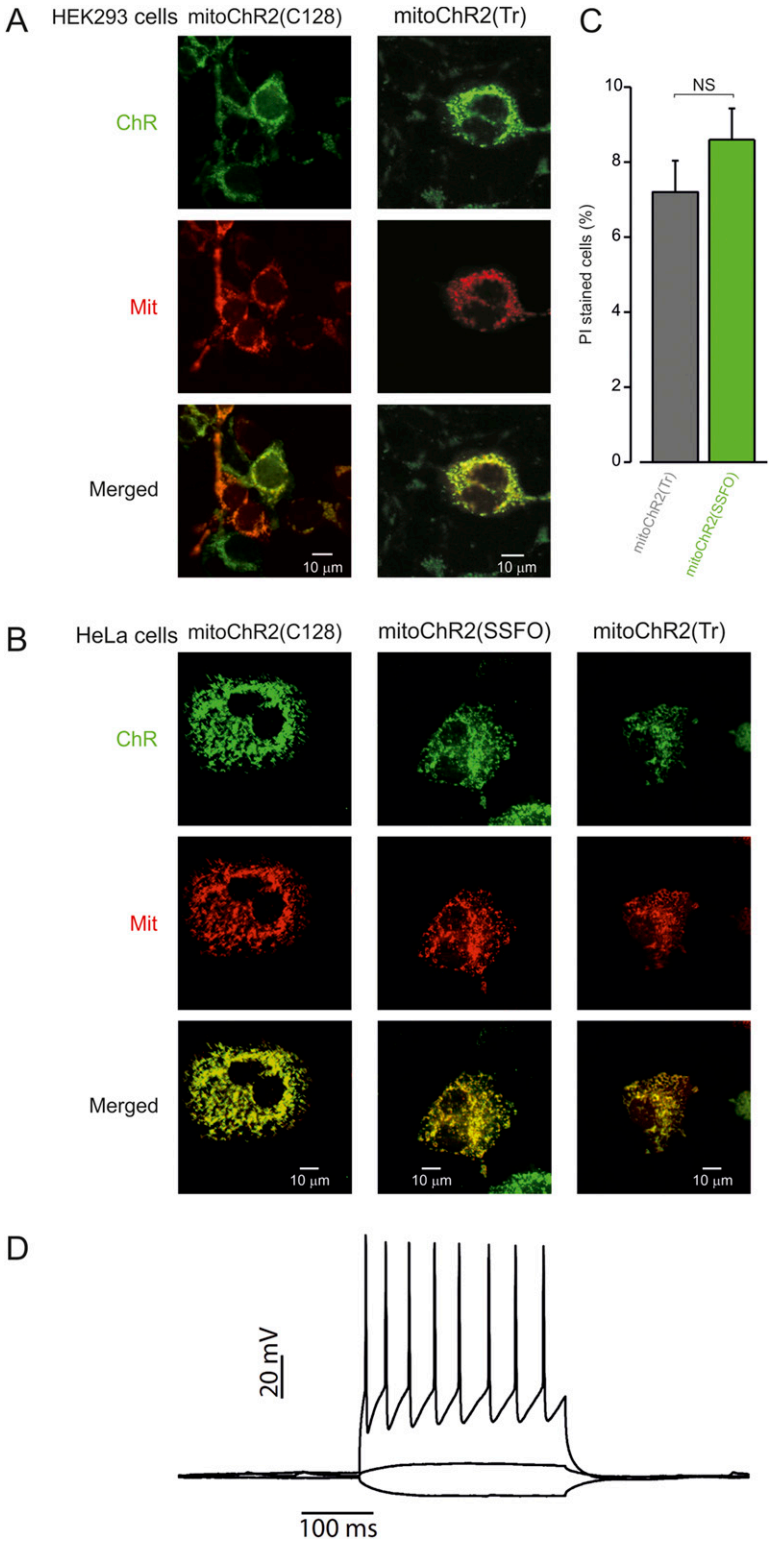

Fig. S1. Mitochondrial localization of mitoChR2 variants in different cell lines. Confocal images of HEK293T (*A*) and HeLa (*B*) cells expressing mitoChR2(SSFO; C128 and truncated) YFP-tagged constructs (green) and Mito-mCherry (red), as indicated. Yellow color indicates colocalization of the mitochondrial marker and the channel. Viability of cells expressing mitoChR2(SSFO) or controls (vector only) that were illuminated for 10 s with blue light (2 mW/mm^2) and stained with PI 30 min after photoactivation. Data are presented as mean ± SEM (*C*). No difference in the number of dead cells was observed ($n > 70$) in cells expressing mitoChR2(SSFO) compared with mitoChR2(Tr). NS, not significant. In control vector transfected cells (*D*), current pulses delivered via the somatic patch pipette elicited either hyperpolarization or repetitive firing, which is similar to those in mitoChR2(SSFO)-expressing neurons (Fig. 1*C*).

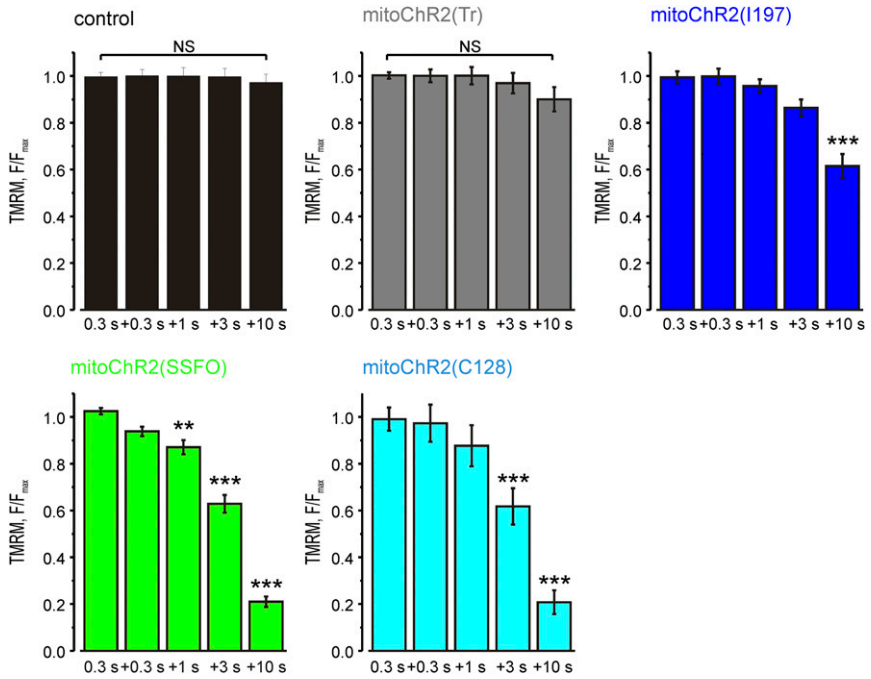

Fig. S2. Quantification of the membrane potential signal changes elicited by light illumination (as marked) in cells expressing the indicated constructs (see representative traces in Fig. 3*A*); $n > 17$ cells for each condition. Data are presented as mean ± SEM. $^{**}P < 0.01$, $^{***}P < 0.001$. NS, not significant.

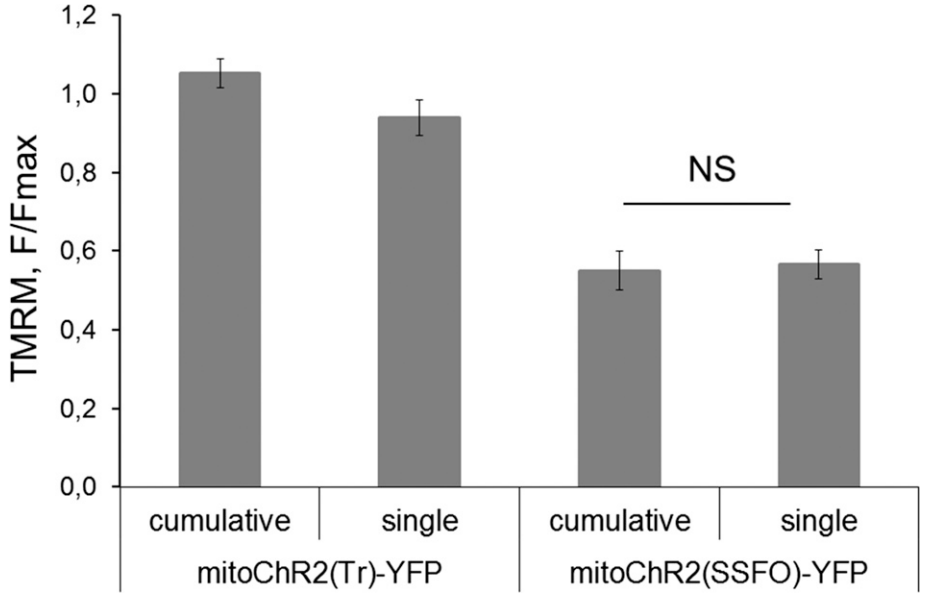

Fig. S3. Effect of a single light pulse or cumulative photoactivation on $\Delta\psi_m$ in HeLa cells. Mean ± SEM F/F_{max} of $\Delta\psi_m$ in HeLa cells expressing mitoChR2(SSFO)-YFP or mitoChR2(Tr)-YFP after 8 min from the first light pulse. Changes in $\Delta\psi$m are elicited by blue light exposures (2 mW/mm^2; bar) for 10-s (single) or by multiple light pulses for 1, 3, and 6 s (cumulative); $n \geq 9$ cells for each condition. NS, not significant.

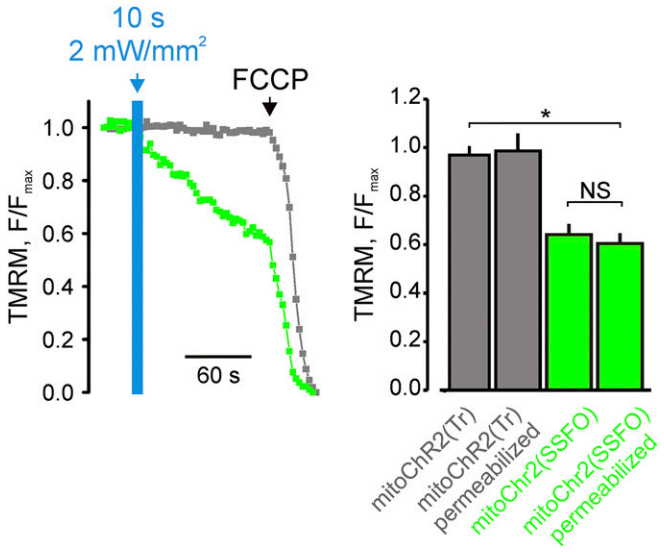

Fig. S4. (*Left*) Light-dependent change in $\Delta\psi_m$ in digitonin-permeabilized HEK293T cells expressing mitoChR2(SSFO) (green) or mitoChR2(Tr) (gray) loaded with TMRM and perfused with intracellular Na^+- and K^+-free solution (*Materials and Methods*). (*Right*) Mean amplitude ± SEM of $\Delta\psi_m$ change in intact or permeabilized cells expressing mitoChR2(SSFO) (green) or mitoChR2(Tr) (gray); $n \geq 71$ cells for each condition. *$P < 0.05$. NS, not significant.

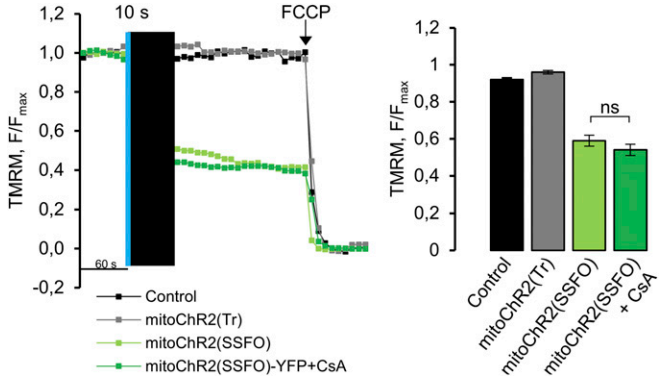

Fig. S5. PTP inhibition does not affect the extent of mitochondrial depolarization induced by mitoChR2(SSFO) opening. Typical traces of single HeLa cells expressing the mitoChR2(SSFO)-YFP variant with or without the addition of the PTP inhibitor CsA (1 μM), void vector-transfected cells, or cells expressing nonfunctional mitoChR2(Tr). The cells were initially illuminated for 10 s with blue light and then kept in the dark for 1 min (black bar) followed by TMRM excitation. The bar graph represents the mean (±SEM; $n \geq 23$ cells per condition) of F/F_{max} changes measured 5 min after the blue light pulse, as described in Fig. 4*C*. NS, not significant.

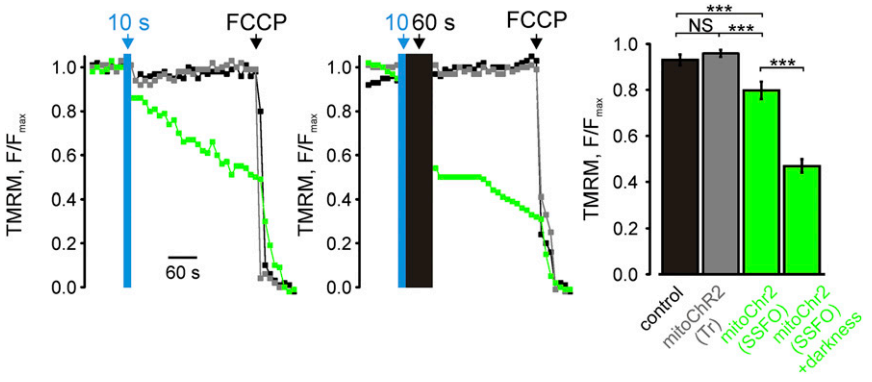

Fig. S6. Effect of TMRM excitation on mitoChR2(SSFO) opening kinetics. Representative kinetics of $\Delta\psi_m$ changes in single HeLa cells expressing mitoChR2(SSFO)-YFP (green trace), mitoChR2(Tr)-YFP (gray trace), or empty vector (coexpressing a mitochondrial YFP; black trace). Where indicated, cells were illuminated with a single 10-s blue light pulse of 2 mW/mm^2 (*Left*) or a single 10-s blue light pulse followed by 60 s of darkness (*Middle*). The bar graph shows mean F/F_{max} changes (±SEM; $n \geq 16$ per condition), calculated 1 min after blue light photoactivation (*Right*). ***$P < 0.001$. NS, not significant.

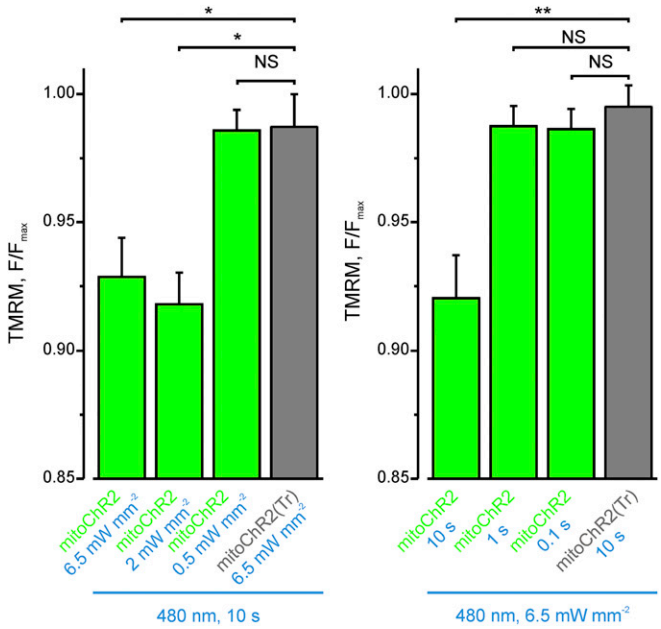

Fig. S7. Light intensity and time dependence of $\Delta\psi_m$ changes in single HEK293T cells expressing mitoChR2 as in Fig. 4C. (*Left*) Light intensity dependence of the indicated mean TMRM F/F_{max} values in mitoChR2(Tr)- (gray bar) and mitoChR2-YFP–expressing cells (green bars); $n \geq 28$ cells per condition. (*Right*) Light time dependence of the indicated mean ± SEM TMRM F/F_{max} values in mitoChR2(Tr)- (gray bar) and mitoChR2-YFP–expressing cells (green bars); $n \geq 85$ cells per condition. $^*P < 0.05$, $^{**}P < 0.01$. NS, not significant.

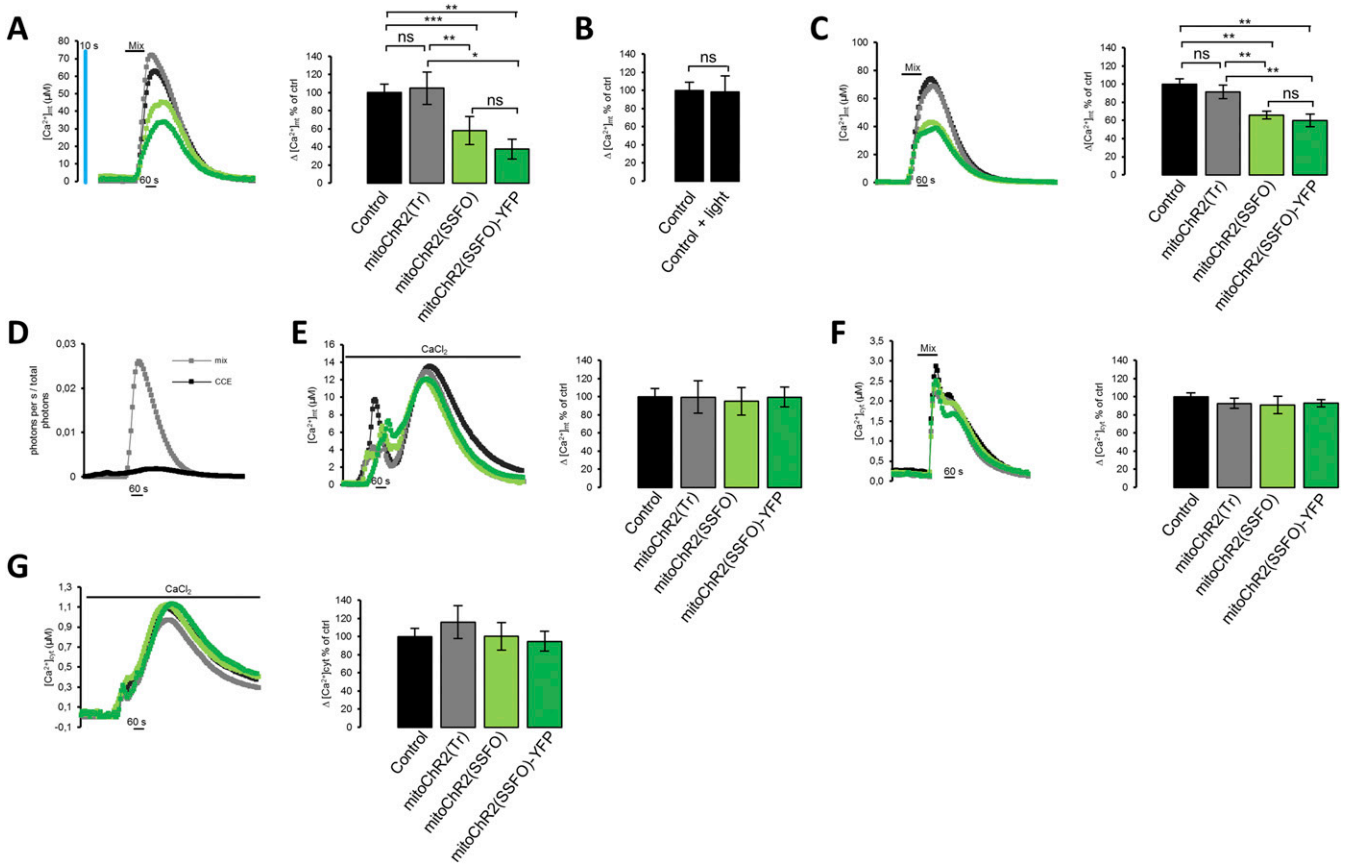

Fig. S8. MitoChR2(SSFO) photoactivation inhibits mitochondrial Ca^{2+} uptake (as measured with targeted aequorin) without inducing intrinsic toxicity. HeLa cells were transiently transfected with empty vector/mitoChR2(Tr)/mitoChR2(SSFO)/mitoChR2(SSFO)-YFP and mt-aequorin (*A*–*E*) or cyt-aequorin (*F* and *G*). (*A*) Cells were analyzed for $[Ca^{2+}]_{mt}$ changes upon the application of a mix of stimuli (histamine, CPA, ATP) after photoactivation of the ChRs with blue light (as described in Fig. 5*A*). (*A*, *Left*) Representative kinetics of $[Ca^{2+}]_{mt}$ in control (black), mitoChR2(Tr)- (gray), mitoChR2(SSFO)- (green), and mitoChR2(SSFO)-YFP– (dark green) expressing cells. (*A*, *Right*) Mean (±SEM; $n \geq 3$ coverslips for each condition) $[Ca^{2+}]_{mt}$ increase normalized to controls. (*B*) The bar graph represents the mean (±SEM; $n \geq 7$ coverslips for each condition) $[Ca^{2+}]_{mt}$ increase normalized to nonpreilluminated controls. (*C*, *Left*) Representative kinetics of $[Ca^{2+}]_{mt}$ in the absence of a blue light pulse when the opening of the channel is triggered by the light emitted locally by aequorin during mitochondrial Ca^{2+} uptake. (*C*, *Right*) Mean (±SEM; $n \geq 3$ coverslips for each condition) $[Ca^{2+}]_{mt}$ increase normalized to controls. (*D*) Typical kinetics of the rates of photon emission during mitochondrial Ca^{2+} uptake induced by the application of a mix of stimuli or by CCE. To activate CCE, cells were first treated with 100 nM thapsigargin in Ca^{2+}-free EGTA containing medium to deplete the stores and then perfused with medium containing 0.75 mM $CaCl_2$, where indicated. (*E*, *Left*) Typical kinetics of the increase in mitochondrial Ca^{2+} concentration ($[Ca^{2+}]_{mt}$) activated by CCE. (*E*, *Right*) Mean (±SEM; $n \geq 7$ coverslips for each condition) $[Ca^{2+}]_{mt}$ increase upon CCE activation, normalized to controls. (*F*) $[Ca^{2+}]_{cyt}$ changes were analyzed upon the application of a mix of stimuli as described in *A*. (*F*, *Right*) Typical kinetics of cytosolic Ca^{2+} increases, $[Ca^{2+}]_{cyt}$. (*F*, *Left*) Mean (±SEM; $n \geq 7$ coverslips for each condition) $[Ca^{2+}]_{cyt}$ increase normalized to control. (*G*) $[Ca^{2+}]_{cyt}$ changes upon the activation of CCE were analyzed as described in *E*. (*G*, *Left*) Representative kinetics of $[Ca^{2+}]_{cyt}$ increase upon CCE activation. (*G*, *Right*) Mean (±SEM; $n \geq 4$ coverslips for each condition) $[Ca^{2+}]_{cyt}$ normalized to control. $^*P < 0.05$, $^{**}P < 0.01$, $^{***}P < 0.001$. NS, not significant.

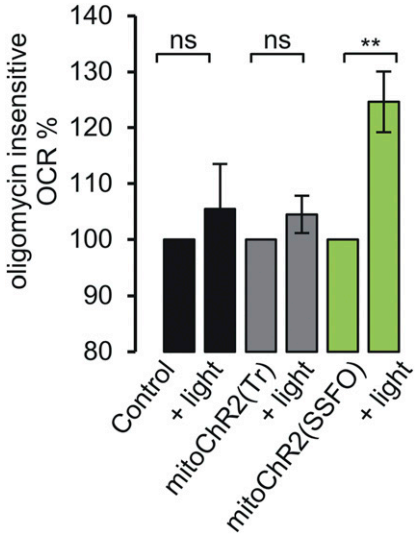

Fig. S9. Blue light-dependent oligomycin-insensitive oxygen consumption. Mean normalized oxygen consumption rate (±SEM; $n \geq 8$ independent experiments) in control (void vector) or mitoChR2(Tr)- or mitoChR2(SSFO)-YFP–transfected HeLa cells. Cells were pretreated with oligomycin, and OCR was measured before and after illumination with a 10-s blue light pulse (*Materials and Methods*). $^{**}P < 0.01$. NS, not significant.

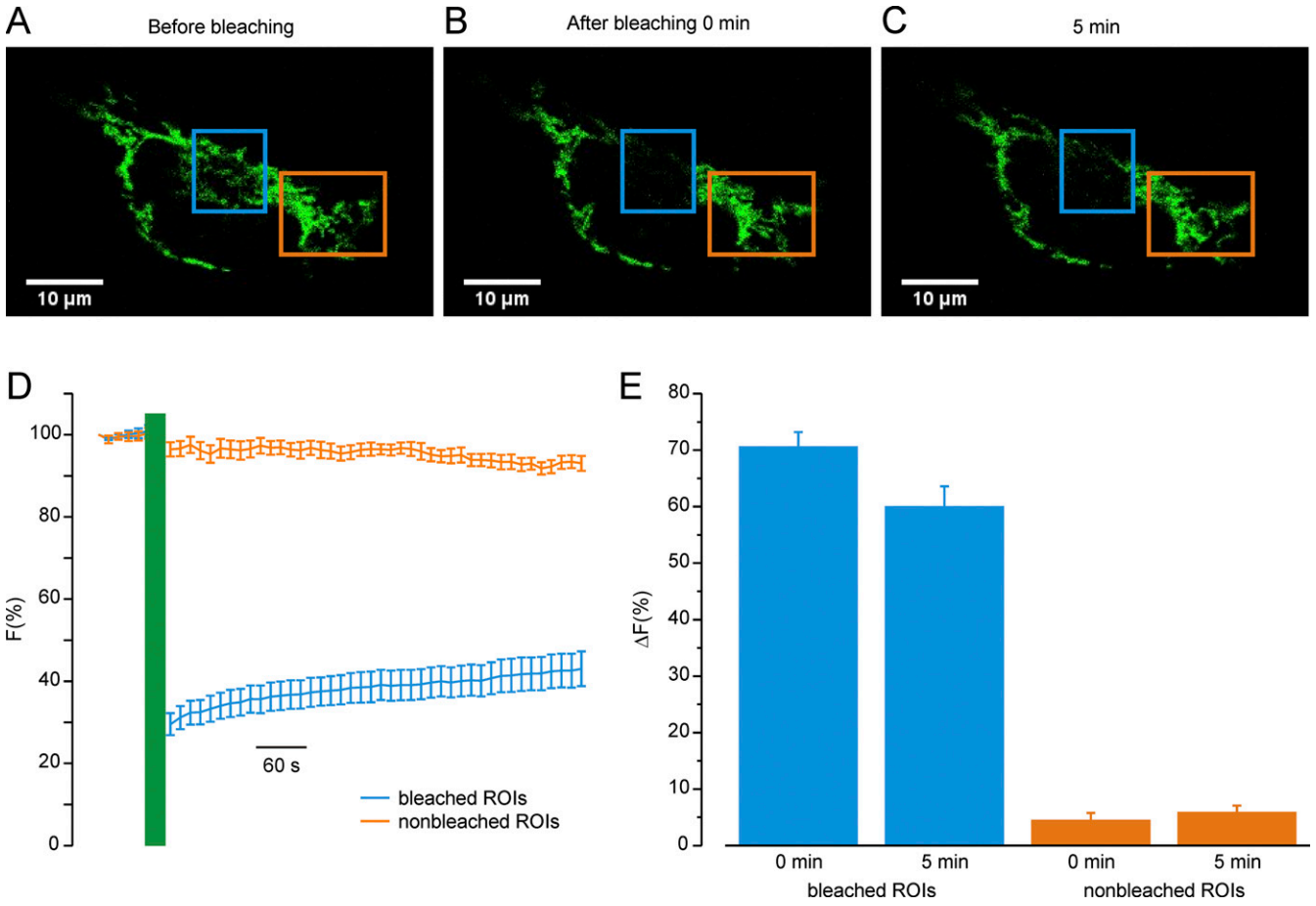

Fig. S10. FRAP analysis of mitochondrial network dynamics. (*A–C*) Representative confocal images of HeLa cells expressing mito-YFP before photobleaching (*A*), immediately after (*B*), and 5 min after (*C*) photobleaching in different regions of interest (ROIs). The blue ROI indicates the bleached area; the orange ROI indicates a nonbleached area. (Scale bars, 10 µm.) (*D*) Mean ± SEM traces of Mito-YFP fluorescence intensity. Traces show fluorescence intensities before and after photobleaching normalized to prebleached ones and plotted over time. The blue trace refers to bleached ROIs; the orange trace refers to ROIs of a nonbleached area. (*E*) Bars represent mean ± SEM values of the $\Delta F(\%)$ changes (calculated as the difference between the fluorescence before bleaching and the fluorescence immediately or 5 min after bleaching) of the indicated ROIs at two different time points: immediately (0 min) and 5 min after bleaching. $n = 12$ cells per condition. $P < 0.05$ between the recovery of bleached and nonbleached regions.

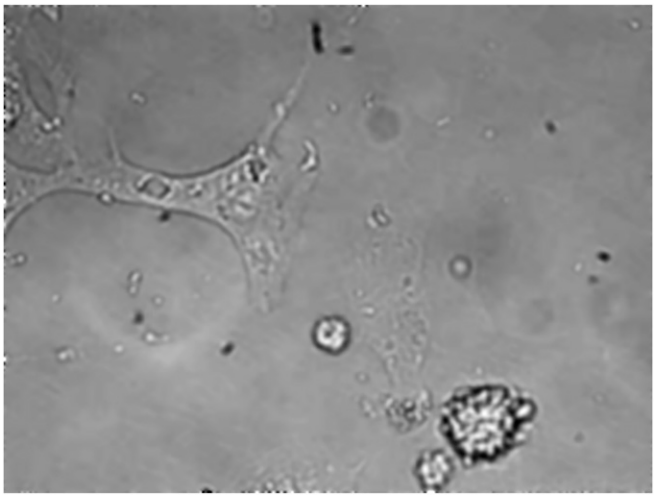

Movie S1. Blue light controls contraction of mitoChR2(SSFO)-YFP–transfected cardiomyocytes. The intermission is blue light illumination.

Movie S1

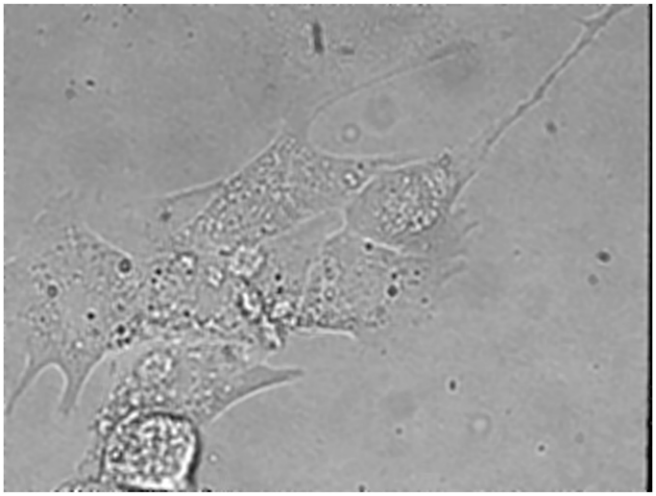

Movie S2. Blue light illumination does not affect the spontaneous beating of cardiomyocytes transfected with mitoChR2(Tr)-YFP. The first intermission is blue light illumination, and the second is application of FCCP (1 μM).

Movie S2

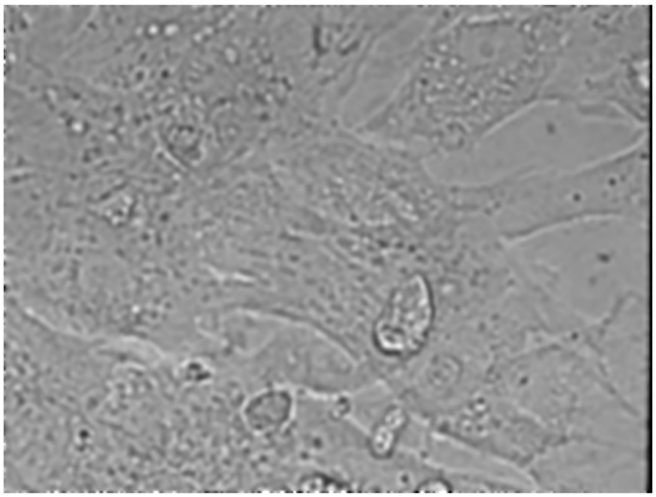

Movie S3. Blue light illumination does not affect the spontaneous beating of cardiomyocytes transfected with Mito-YFP. The first intermission is blue light illumination, and the second is application of FCCP (1 μM).

Movie S3